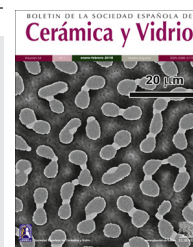




BOLETIN DE LA SOCIEDAD ESPAÑOLA DE  
**Cerámica y Vidrio**

www.elsevier.es/bsecv



## Alkali activated slag cements using waste glass as alternative activators. Rheological behaviour



Manuel Torres-Carrasco,\* Carlos Rodríguez-Puertas, María del Mar Alonso, and Francisca Puertas

Eduardo Torroja Institute for Construction Sciences (IETcc-CSIC), Madrid, Spain

### ARTICLE INFO

#### Article history:

Received 19 January 2015

Accepted 25 February 2015

#### Keywords:

Waste glass

Alternative activators

Alkali-activated materials

Rheology

Yield stress

### A B S T R A C T

The purpose of this study is to investigate new activators in the preparation of alkali-activated materials (AAMs) alternative to Portland cements by reusing waste glass. Alkali-activated blast furnace slag (AAS) constitutes an alternative to Portland cement due to high energy and environmental pollution associated with industrial Portland cement. Moreover, alkali activated materials offer a series of higher properties than ordinary Portland cement (OPC), such as better strength and durability behaviour. However, the rheology of these materials has been much less intensely researched.

The present study aimed to study the effect of waste glass as activator and as replacement of blast furnace slag on the rheological behaviour of AAS pastes, with a comparison between the rheological parameters and fluidity of these pastes to the same parameters in standard cements (CEM I and CEM III/B).

The findings show that AAS paste behaviour of rheology when the activator was a commercial waterglass solution or NaOH/Na<sub>2</sub>CO<sub>3</sub> with waste glass was similar, fit the Herschel-Bulkley model. The formation of primary C-S-H gel in both cases were confirmed. However, the rheological behaviour in standard cements fit the Bingham model. The use of the waste glass may be feasible from a rheological point of view in pastes can be used.

© 2015 Sociedad Española de Cerámica y Vidrio. Published by Elsevier España, S.L.U.

This is an open access article under the CC BY-NC-ND license

(<http://creativecommons.org/licenses/by-nc-nd/4.0/>).

### Preparación de cementos de escoria activada alcalinamente utilizando residuos vítreos como activador alcalino. Comportamiento reológico

### R E S U M E N

El propósito de este estudio es investigar nuevos activadores alcalinos a través de la reutilización de residuos vítreos en la preparación de materiales activados alcalinamente alternativos al cemento Portland (OPC). Las escorias activadas alcalinamente (AAS) son una alternativa al cemento Portland debido a la alta demanda energética y medioambiental

#### Palabras clave:

Residuos vítreos

Activadores alternativos

Materiales activados alcalinamente

\* Corresponding author.

E-mail: mtorres@ietcc.csic.es (M. Torres-Carrasco).

Reología  
Esfuerzo umbral

asociada en la producción de este. Además, estos materiales activados alcalinamente ofrecen mejores propiedades que el cemento Portland, como un buen comportamiento mecánico y durable. Sin embargo, el comportamiento reológico de estos materiales ha sido poco investigado.

El presente estudio tiene como objetivo estudiar el efecto del residuo vítreo como activador y como sustitución de la escoria en el comportamiento reológico de las pastas, con una comparación entre los parámetros reológicos y de fluidez de estas pastas frente a los mismos en los cementos normalizados (CEM I and CEM III/B).

Los resultados reológicos de las pastas de escoria activada alcalinamente cuando los activadores fueron una disolución comercial de waterglass y NaOH/Na<sub>2</sub>CO<sub>3</sub> con el residuo vítreo presentaron un comportamiento muy similar, describiendo un modelo Herschel-Bulkley, en donde se confirmó la formación de un gel C-S-H primario en ambos casos. Sin embargo, el comportamiento reológico en los cementos normalizados describe un modelo Bingham. El uso de un residuo vítreo puede ser factible desde un punto de vista reológico en las pastas de escoria activadas alcalinamente.

© 2015 Sociedad Española de Cerámica y Vidrio. Published by Elsevier España, S.L.U.

This is an open access article under the CC BY-NC-ND license (<http://creativecommons.org/licenses/by-nc-nd/4.0/>).

## Introduction

Portland cement (OPC) is considered the excellence building material because there is not binder that holds the acceptance that has this material. This is due to its high performance, its good quality/price ratio and because it is possible to find the raw materials to produce it almost anywhere in the world. However, the production of Portland cement is considered a complex and highly intensive process as far as energy is concerned, from the use of raw materials to the production and grinding of clinker.

Additionally, the cement industry is considered one of the industries that emit larger amounts of CO<sub>2</sub> into the atmosphere worldwide. In the manufacturing process about 900 kg of CO<sub>2</sub> per tonne of cement produced are emitted [1,2], being approximately 5-7% of global emissions caused by humans [3]. The main CO<sub>2</sub> emissions in the cement industry come directly from the combustion of fossil fuels and the calcination of limestone into calcium oxide. An indirect amount of CO<sub>2</sub> comes from the consumption of electricity generated by burning fossil fuels and milling processes. Approximately around 33% of CO<sub>2</sub> emissions are originated from the fuel and the rest originates from the calcination of limestone (66%) [4]. The mass balance results in emissions

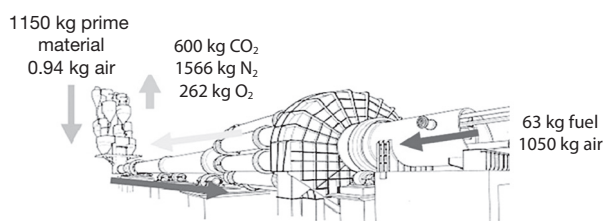


**Fig. 1 – Mass balance in a typical production process of cement [5].**

of CO<sub>2</sub> and other gases in the production of Portland cement is shown in Figure 1 [5].

At this time reducing CO<sub>2</sub> is the most important environmental objective worldwide to reduce the atmospheric concentration of greenhouse gases. Between 2000 and 2006 CO<sub>2</sub> emissions increased by 54% worldwide [6]. Since 2006 and due to population growth and global demand of concrete as the main building material for construction, also cement production expected to increase in each year between 0.8-1.2% to 3.7-4.4 billion tonnes in 2050. As a result of this significant growth in cement production, CO<sub>2</sub> emissions will also strongly increase. While global CO<sub>2</sub> emissions in a cement plant in 1990 were 576 million tons [7], emissions tripled and reached 1.88 billion tons in 2006. If this tendency continues without any measures that might curb the amount of CO<sub>2</sub> into the atmosphere due only to cement industry, will become 2.34 billion tons in 2050 [6].

All these possible upcoming events have urged to industry and governments to devote time to study and implement various different promising strategies to reduce the accumulation of emissions of greenhouse gases in the atmosphere. The Kyoto Protocol and the Copenhagen conference were the last overall efforts of the United Framework Convention on climate change. Under these agreements some countries decided to reduce their greenhouse gases [8].

Due to some of the environmental problems associated with the production of Portland cement emerge some alternative to try to obtain the sustainable development, for instance, through technological progress in the cement plants; using alternative materials (waste and industrial by-products) as partial or complete replacements for oil, fuel, raw materials or clinker (cement with additions) or across the development of new cementing materials more eco-efficient.

Some of these alternative type cements are those resulting from the chemical interaction between strongly alkaline solutions or amorphous aluminosilicates, which can be natural or industrial wastes such as fly ash or blast furnace slag [9-12]. The alkaline solutions used in this process are usually: alkaline metal or alkaline-earth hydroxides (ROH, R(OH)<sub>2</sub>); weak acid salts (R<sub>2</sub>CO<sub>3</sub>, R<sub>2</sub>S, RF); strong acid salts (Na<sub>2</sub>SO<sub>4</sub>,

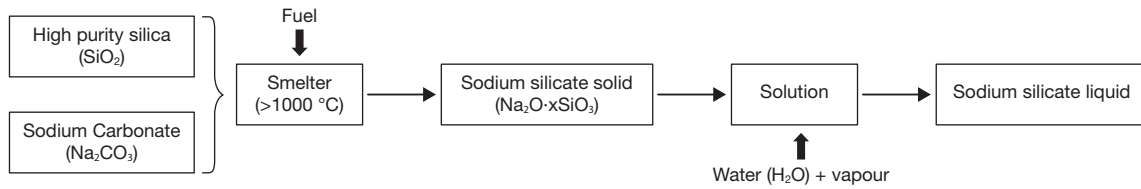


Fig. 2 – Commercial manufacturing process of sodium silicate.

$\text{CaSO}_4 \cdot 2\text{H}_2\text{O}$ ); and  $\text{R}_2\text{O}(n)\text{SiO}_2$ -type siliceous salts, where R is an alkaline ion such as Na, K or Li. From the standpoint of resistance and durability of the final products formed, the most effective solutions are NaOH,  $\text{Na}_2\text{CO}_3$  and hydrated sodium silicates or waterglass solutions [13-16].

The hydrated sodium silicates (waterglass) have provided optimal mechanical resistance in alkali activated materials (AAMs) and good durability. The  $\text{SiO}_2$  present in the chemical composition of these activators causes the final reaction products to have special characteristics compared to other activators [11,17]. These sodium silicates are inorganic chemical compounds produced from combination, in varied proportions, of purity silica salts ( $\text{SiO}_2$ ) and sodium carbonate ( $\text{Na}_2\text{CO}_3$ ). The fusion of these materials at temperatures above  $1000\text{ }^\circ\text{C}$  causes the solid sodium silicate ( $\text{Na}_2\text{O} \cdot x\text{SiO}_3$ ) as an amorphous glass [18,19] (Fig. 2). This solid silicate is then dissolved in water to obtain the soluble or liquid silicate, which is used in various industrial applications. However, this industrial process is extensively criticized because it is a highly polluting process from an environmental ( $\text{CO}_2$  emissions) and energy point of view, due to high temperatures used to bring about the fusion [18,19]. The estimated results of  $\text{CO}_2$  emissions in the production of sodium silicates are shown in Table 1, where we can observe that the total emissions estimate is around 1.514 kg of  $\text{CO}_2$  per kilogram of sodium silicate produced [20]. However, it is important to note that this study does not include energy expended during the extraction of raw materials so that actual emissions of  $\text{CO}_2$  are likely that are greater than the estimate provided of 1.514 kg  $\text{CO}_2$ .

The motivation of this work is to try to get new sodium silicates through the reuse of waste glass. The urban and industrial waste glasses are an amorphous material with a chemical composition consisting essentially of  $\text{SiO}_2$  (65-75%), CaO (6-12%),  $\text{Na}_2\text{O}$  (12-15%),  $\text{Al}_2\text{O}_3$  (0.5-5%) y  $\text{Fe}_2\text{O}_3$  (0.1-3%), attempting to replace as much as possible the commercial activator (waterglass) employed to the present [15].

Glass is an ideal material to be recycled, as once recycled, their use can help save energy in preparing new glasses due to it requiring 26% less energy, needed less expensive and reduces raw materials employed in the preparation of glasses. However, there is a percentage between 10-30% of these waste glasses are not re-allocated to the preparation of new glass containers because they have some kind of impurities either metal or ceramic type. The construction sector plays an important role in the reuse of this percentage of waste glass, using them as pozzolanic additions in the preparation of Portland cement; in the preparation of vitroceraamic composites together with other industrial waste or by-products, such

as fly ash, slag and ceramic discards; or as a prime material for synthesizing solid sodium silicates or purified silica. In this later application, very recent research by our group [14,15,21-23] have shown that sodium silicate-based urban waste glass may serve as an active component in the preparation of alkali-activated slag (AAS) or fly ash (AAFA) cements. The optimal conditions of solubility and concentration of ions, mainly  $\text{SiO}_2$  and  $\text{Al}_2\text{O}_3$ , have been established, which allowed us to use these solutions as an alternative activator in the preparation of alkali activated slag or fly ash pastes [14,15,24].

Alkali activated slag (AAS) or fly ash (AAFA) cements and concretes offer a series of better properties than an ordinary Portland cement (OPC), such as high levels of resistance to short and long times and an excellent durability behaviour in the face of chemical and physical agents, etc. An assessment of recent environmental life cycle [25] shows that concretes prepared based on alkali activated slag have a 73% less greenhouses gas emissions, 43% less of energy is required, 25% less water and values about 22-94% less than several parameters related to the toxic environmental impact compared to OPC concrete values.

Table 1 – Estimates of emissions arising due to sodium silicate manufacture [20].

	Emissions arising from energy expended during manufacturing	
	Energy flow (MJ/1000 kg)	Emissions (kg $\text{CO}_2$ /kg)
Electricity	3118	1.065
Coal	296	0.027
Oil (heavy)	9	0.001
Oil (average/light)	456	0.033
Diesel oil	144	0.010
Gas	1270	0.076
Others	78	0.009
Total	5371	1.222
	Emissions caused by transport	
	Air emissions (kg/1000 kg)	Emissions (kg $\text{CO}_2$ /kg)
Carbon dioxide ( $\text{CO}_2$ )	288.7	0.289
Methane ( $\text{CH}_4$ )	0.128	0.003
Total		0.292
Grand total (kg $\text{CO}_2$ /kg)		1.514

The rheological behaviour of pastes, mortars and concretes of Portland cement is well known due to the rheology of these systems has been studied thoroughly. However, studies on the rheological behaviour in alkali activated pastes, mortars and concretes are still scarce. Stryczek and Gonet [26] conducted a preliminary study of the rheological behaviour of alkali activated slag pastes with sodium carbonates. Subsequently, Palacios et al. [27] studied the rheological behaviour in alkali activated slag pastes and mortars with the addition of organic additives. Through this study found that the pastes activated with NaOH fit the model of Bingham; whereas those prepared with the waterglass solution is better positioned to Herschel-Bulkley model [28,29].

Nevertheless, there are still many unknowns to solve regarding the rheological behaviour of alkali activated slag systems. Furthermore, no studies concerning the rheological behaviour of a system of alkali activated slag using solutions from waste glass as replacement of waterglass solution.

With this work we want to show that the use of waste glass as activator in aluminosilicate materials can originate systems with very similar mechanical performance than when a commercial sodium silicate (waterglass) is used and in turn, we want to check what is the rheological behaviour of these alkali activated materials and compared with results obtained with standard Portland cements.

## Experimental program

### Characterisation of materials

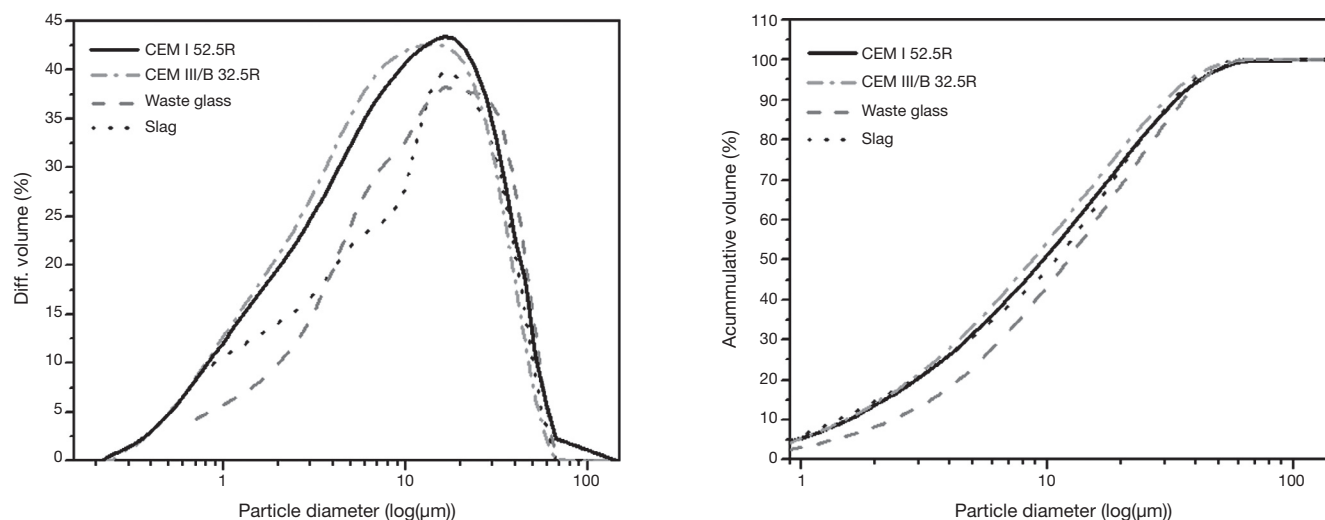
Table 2 gives the chemical composition of the vitreous blast furnace slag (from ENSIDESA factory, Avilés-Spain), the waste glass (from Ajalvir plant, Madrid-Spain) and the standard cements used in this study. The Spanish vitreous blast furnace slag have a vitreous phase accounted for 99% of the slag content and specific surface of this material was 325 m<sup>2</sup>/kg (EN 196-6). The chemical composition of the waste glass show that the majority oxides present in this type of waste are SiO<sub>2</sub>, Na<sub>2</sub>O and CaO. As reference, we used two types of standard cements, CEM I 52.5R and CEM III/B 32.5R (cement with high content of blast furnace slag) where the results obtained by XRF (PHILIPS PW-1004 X-RAY) match which chemical specifications of each of the cements.

Figure 3, in turn, shows the particle size distribution of slag, waste glass and the standard cements used in this work (an analyzer Helos 12K of Sympatec mark was used. Samples were analyzed suspended in isopropyl alcohol with an ultrasonic time of 60 s and measurement time of 15 s). According to these results, the particle size distribution of slag and waste glass provided a single mode and they are below 10%,

**Table 2 – Chemical composition of slag, waste glass and standard cements (wt.%) determined by XRF.**

wt.%	CaO	SiO <sub>2</sub>	Al <sub>2</sub> O <sub>3</sub>	MgO	Fe <sub>2</sub> O <sub>3</sub>	S <sup>2-</sup>	SO <sub>3</sub>	Na <sub>2</sub> O	K <sub>2</sub> O	L.O.I*
Slag	41.00	35.54	13.65	4.11	0.39	1.91	0.06	0.01	-	2.72
Waste glass	11.75	70.71	2.05	1.17	0.52	-	-	11.71	1.08	0.83
CEM I 52.5R	57.05	20.51	5.37	3.86	2.10	-	6.37	0.64	1.44	2.35
CEM III/B 32.5R	49.25	29.91	7.80	6.33	0.95	1.2	1.01	0.33	0.38	2.44

\* L.O.I = Loss on ignition.



**Fig. 3 – Standard cements, slag and waste glass particle size distribution.**

50% and 90% are shown in Table 3. It is important to note that in this study, a waste glass was used with particle size under 45 microns, as in previous studies [15] it was found as with this particle size the results were better. Rather, standard cements CEM I 52.5R and CEM III/B 32.5R had a size distribu-

tion similar in both cases but in this case with the existence of two modes of particle size distribution. Particle sizes under 10%, 50% and 90% are shown in Table 3.

The characterization of the starting materials through FTIR and XRD techniques can be seen in Figure 4 and Figure 5 respectively. The FTIR spectra were obtained by analysing KBr pellets containing 1.0 mg of sample in 300 mg of KBr on a Nicolet 6700 Thermo FTIR spectrometer. The spectra were recorded after running 64 scans in the 4000-400  $\text{cm}^{-1}$ .

% volume	Particle diameter ( $\mu\text{m}$ )			
	CEM I 52.5R	CEM III/B 32.5R	Slag	Waste Glass
10	1.76	1.88	1.41	2.34
50	9.49	12.61	10.89	12.20
90	29.34	42.03	32.67	35.78
Specific surface ( $\text{m}^2/\text{kg}$ )	481	393	325	-

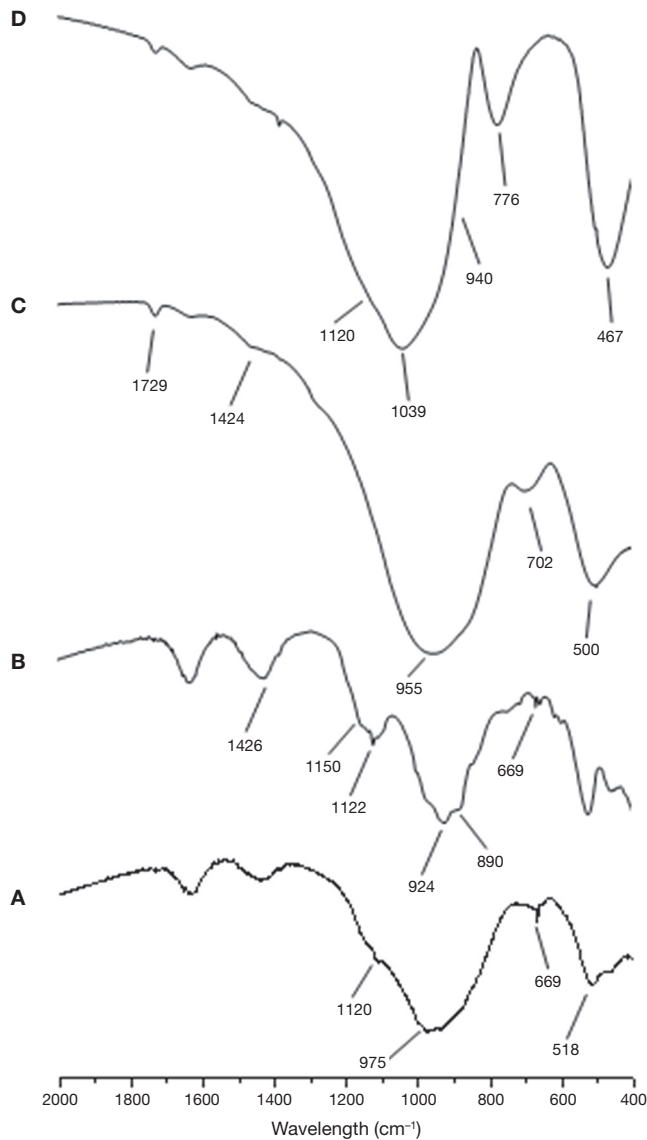


Fig. 4 – FTIR spectra for raw material used: A) CEM III/B 32.5R; B) CEM I 52.5R; C) blast furnace slag; D) waste glass.

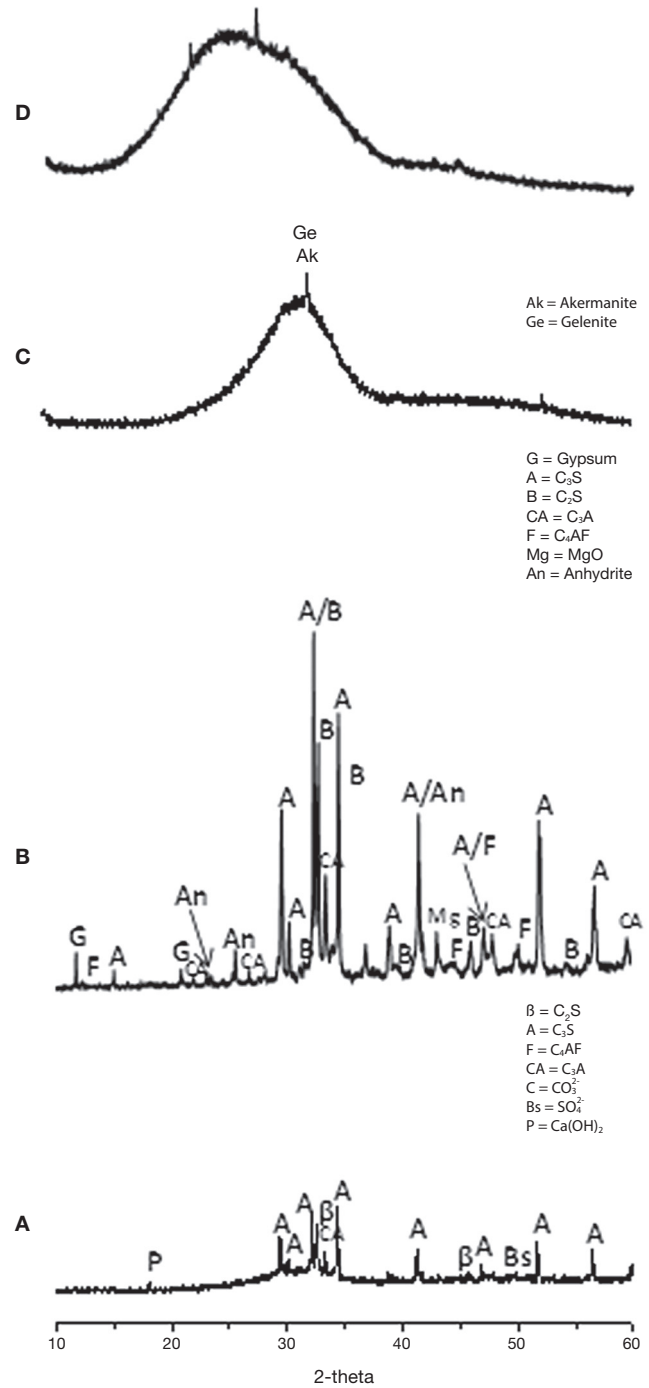


Fig. 5 – XRD patterns for raw material used: A) CEM III/B 32.5R; B) CEM I 52.5R; C) blast furnace slag; D) waste glass.



The XRD patterns for the samples were recorded on a Bruker AXS D8 Advance diffractometer fitted with a Lynxeye super speed RX detector, a 2.2-kW Cu anode no monochromator. The scanning range, from 5 to 60° was covered in a 24-minute period. The instrument was set at 40 kW and 30 mA and the sample was not rotated during scanning.

The FTIR spectrum corresponding to the sample CEM I 52.5R (Fig. 4A) shows as majority phase  $C_3S$  with  $C_2S$ ,  $C_3A$  and  $C_4AF$ . The bands are observed at 924  $cm^{-1}$  and from 874–890  $cm^{-1}$  correspond to the deformation vibration of silicate tetrahedrons (O-Si-O) of the alite and belite phases. Between 600 and 800  $cm^{-1}$  were observed several bands corresponding to the vibration of  $AlO_6$  distorted octahedral. In the range 1132–1148  $cm^{-1}$  and 1098–1121  $cm^{-1}$  two bands associated with asymmetric stretching vibration of the sulfate groups ( $SO_4^{2-}$ ), due to the gypsum incorporated into the clinker cement are presented. Finally, the band around 1426  $cm^{-1}$  corresponds to the asymmetric stretching vibration of carbonates due to the presence of limestone or environmental  $CO_2$  carbonation cements (weathering) [30,31]. With respect to the spectrum of CEM III/B 32.5R (Fig. 4B) a signal is observed at 975  $cm^{-1}$  as a wider band due to the presence of blast furnace slag in the cement. Furthermore, the presence of low intensity bands are detected at intervals 1132–1148  $cm^{-1}$  and 1098–1121  $cm^{-1}$  associated with the stretching vibration of the sulfate groups  $\nu_3$  ( $SO_4^{2-}$ ).

In the case of the vitreous slag, the FTIR spectrum (Fig. 4C) shows a broad band at 850–1050  $cm^{-1}$  characteristics of the asymmetric stretching vibration of Si-O in the silicate tetrahedrons. The vibration band appears at 472  $cm^{-1}$  is assigned to deformation vibrations of silicate tetrahedrons,  $\nu_4$  (O-Si-O), while between 600–800  $cm^{-1}$  band is located corresponding to the asymmetric stretching vibration of Al-O bonds of  $AlO_4$  slag groups. The bands appear to 1418  $cm^{-1}$  is assigned to asymmetric stretching vibration  $\nu_3$  ( $CO_3^{2-}$ ) indicating the partial carbonation of the anhydrous slag.

Regarding the FTIR spectrum for waste glass, we can see in Figure 4D family and characteristics bands with silicates chains found in the central region of the spectrum. The signal appearing at 460–480  $cm^{-1}$  corresponds to the stretching vibrations of the Si-O-Si and that signal is very sharp. Around 775–800  $cm^{-1}$  a sharp signal appears corresponding to the symmetric stretching vibrations of the bonds O-Si-O. Acute and wide band appears in the region of 1040  $cm^{-1}$ , which corresponds to the asymmetric stretching vibration and oxygen bridges. Moreover, this signal can be seen two small shoulders, one around 940  $cm^{-1}$  (corresponding to vibration of the non-bridging oxygen) and a shoulder at around 1120  $cm^{-1}$  (asymmetrical vibration of Si-O-Si of oxygen bridges). The signal appearing at 1460  $cm^{-1}$  is due to carbonate groups existing in the glass.

From the XRD results (Figs. 5A and 5B) can be extracted as the majority crystalline phase used in all cements is the  $C_3S$  or alite. It is important to note that CEM III/B 32.5R cement has a content of amorphous material of 70.27% corresponding to the vitreous blast furnace slag, coinciding with the specifications provided by the supplier of this cement and according to the type of cement to in accordance with UNE EN 197-1:2000 [32].

Slag XRD diffractogram (Fig. 5C) exhibits high amorphous content with a maximum around  $2\theta=30-32^\circ$  and only very minor contents of crystalline phases of highest intensity, like gehlenite ( $2\theta=31.42^\circ$ ,  $29.13^\circ$  y  $52.09^\circ$ ) and akermanite ( $2\theta=31.14^\circ$ ,  $28.87^\circ$  y  $51.78^\circ$ ) appear constituting the slag.

The XRD mineralogical characterisation (Fig. 5D) shows the glass to be an amorphous material, with low range structural order. No peaks attributed to any crystallised compound can be identified except a broad diffraction halo, which is attributed to the glassy phase. The position of the diffraction halo is related to the lime content and sodium content in the glass [33–36].

#### Pastes preparation and test conducted

Rheological parameters and fluidity of pastes over time were determined by means of rotational viscosimeter trials and Minislump tests respectively.

The tests were performed for the following cement pastes (see Table 4):

- Commercial standard cements (CEM I 52.5R and CEM III/B 32.5R) used as a reference.
- A vitreous blast furnace slag (BFS) activated with a commercial waterglass solution (Merck, 27%  $SiO_2$ ; 8%  $Na_2O$  and 65%  $H_2O$  by weight) with a constant concentration of 5%  $Na_2O$  by mass of slag (AAS WG).
- A vitreous blast furnace slag activated with 50% wt. NaOH/ $Na_2CO_3$  solution with the waste glass (25 g per 100 mL of solution) with a constant concentration of 5%  $Na_2O$  by mass of slag (AAS N/C-waste glass). The process of waste glass treatment for obtaining the alternative activator has been explained in previous studies [14,15].
- A vitreous blast furnace slag activated with 50% wt. NaOH/ $Na_2CO_3$  solution (5%  $Na_2O$  by mass of slag) with waste glass, with a substitution of 10% of the slag by the residual glass waste obtained after solubility process (AAS N/C-glass+10%).

The liquid/solid ratios used in the rheological testes are shown in Table 4. In all cases the consistencies were similar according to standard UNE 80-116-86.

**Table 4 – Physical and chemical characteristics of the solutions and sample labelling.**

Sample name	Activator type	$SiO_2/Na_2O$	L/S
AAS WG	Commercial waterglass	0.86	0.55
AAS N/C-glass	NaOH/ $Na_2CO_3$ + waste glass	0.86	0.55
AAS N/C-glass+10%	NaOH/ $Na_2CO_3$ + waste glass + 10% residual glass waste	0.86	0.55
CEM I 52.5R	Water	-	0.45
CEM III/B 32.5R	Water	-	0.35

### Variation in shear stress pastes at a constant shear rate

Prior to the introduction of pastes in the viscometer, the pastes were prepared by mechanically stirring a mix of 80 g of binder (cement or blast furnace slag) with a liquid/solid ratio fixed (see Table 4) for 3 min. In the case of the pastes with the replacement of blast furnace slag by the solid residue of the waste glass (10% wt) after attack with NaOH/Na<sub>2</sub>CO<sub>3</sub>, the solids were premixed before paste preparation. All pastes were tested for 30 min on a Haake Rheowin Pro RV1 rotational rheometer fitted with a serrated cylindrical rotor and operating at a constant shear rate of 100 s<sup>-1</sup>.

### Determination of rheological parameters: yield stress

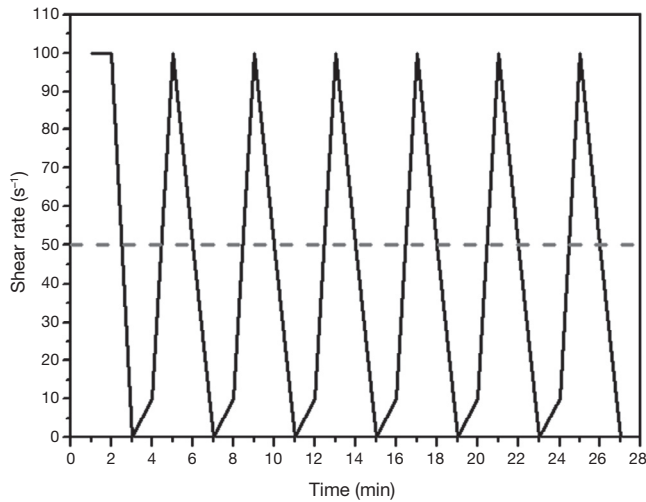


**Fig. 6 – Dynamic rheological testing with standard Portland cements and AAS pastes.**

Paste rheological behaviour was characterised by determining yield stress, using the aforementioned rotational rheometer. The procedure consisted of pre-shearing at 100 s<sup>-1</sup> for 2 min, followed by ramping up from 0 to 10 s<sup>-1</sup> in 1 min and from 10 to 100 s<sup>-1</sup> in 1 min and then ramping down from 100 to 50 s<sup>-1</sup> in 1 min and from 50 to 0 s<sup>-1</sup> in 1 min. This cycle was repeated six times, with 5-sec pause in between cycles [28,37]. The test procedure is depicted in Figure 6. The yield stress and plastic viscosity values used in the calculations were the means of at least three trials conducted on pastes activated with the same solution.

### Paste fluidity (Minislump test)

Paste fluidity was determined with the Minislump test [38]. The pastes were prepared in a mixer (Ibertest Autotest 200/10) first for 1.5 min at low speed (140 rpm) and after a 30-s pause, for 1.5 min at high speed (285 rpm). At the specified times, the pastes were placed in a truncated cone measuring 190×381×572 mm, which was the capsized and emptied. The pastes were dropped 10 times on a flow table and the diameter was measured in three directions: the values used were the arithmetic means of these measurements. The pastes were prepared with 500 g of solid (cements or blast furnace slag or residue solid of waste glass and slag) and the same liquid/solid ratio used for rheological measurements.

## Results and discussion

### Variations in shear stress in AAS pastes at a constant shear rate

In the CEM I 52.5R paste (Fig. 7A), once introduced into the viscometer, the shear stress value initially reaches 300 Pa to experience low steep up stress of 100 Pa to 420 seconds after to start of trial to remain constant. This is because in this cement, hydration effect causes some initial flocs responsible

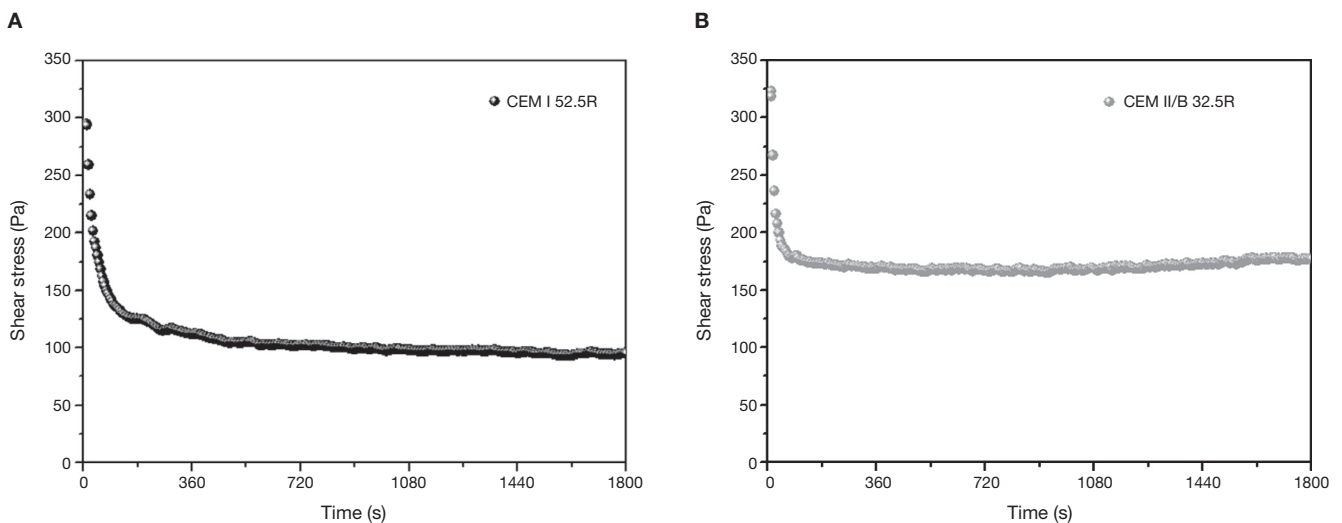


**Fig. 7 – Shear stress vs time in standard cements: A) CEM I 52.5R and B) CEM III/B 32.5R.**

for higher initial values of shear stress, around 300 Pa. As a result of constant rotation, these flocs are broken resulting a fluid paste with the corresponding decrease in shear stress values.

Due to the difference in chemical composition between the CEM I 52.5R and CEM III/B 32.5R, where the latter has a content of amorphous phase of 70% corresponding to the addition of blast furnace slag, is a factor determining to explain the results corresponding to its rheology. In this case it is shown that stress values are very similar to those of CEM I 52.5R pastes (Fig. 7B). However, the shear stress values have a descent more pronounced, reaching the stability in just 90 seconds with a value of about 175 Pa, where these shear stress values are 75% higher than CEM I pastes values.

High stress values are due to the morphology of the slag grains, which have an structure with a greater number of edges, giving to the paste these high shear stress values. Moreover, the rupture of the flocs is faster in this case because the hydration in these pastes is much lower than in Portland cement, resulting fewer hydration products than in CEM I 52.5R pastes. The effect of addition of blast furnace slag percentage in the rheology of the pastes was studied by Palacios et al. [39] where it was found that with a higher percentage of addition, the pastes showed higher values of normal shear stress.

When slag pastes are activated with different activators used in this study, the rheological behaviour depends on the type of activator used (Fig. 8A). When the activator was a commercial waterglass solution, the behaviour of this paste was peculiar because there is a case of "false setting". In this case the initial values of shear stress is lower (78 Pa) than in previous cases. In the early stages of hydration/activation exist a drop in the values of stress to make way then a rapid increase thereof, reaching its maximum value to 420 seconds after starting the test, with a value of 60 Pa. It reaches this maximum; a decrease of 33% in the values of stress exists in this type of pastes to stabilize at 40 Pa to 900 seconds after starting the test. According to the literature [40,41], the slag grains immediately after contact with the solution are surrounded by a thin layer of primary C-S-H gel from interaction between silicate ions from sodium silicate solution with  $\text{Ca}^{2+}$  ions from the blast furnace slag. In this situation the slag grains are bonded by Van der Waals force larger flocs. During the early stages of rheological testing these flocs are partially separated but rapid and massive precipitations of C-S-H primary gel continuous and form flocs larger. In the experimental conditions used, the constant stirring of the sample causes the breakage of flocs, which explains the decrease in shear stress causing that the paste flow. According to previous studies [28,39,41,42] once exceeded the threshold value, total disruption of the structure of the flocs and the consequent decrease of the shear stress values are detected to keep these constant.

When the activating solution used was  $\text{NaOH}/\text{Na}_2\text{CO}_3$  with the waste glass (AAS N/C-glass) [14], the values of shear stress obtained at constant shear rate reflected a very different rheological behaviour. The initial shear stress value reaches a value of 112 Pa, down to 70 seconds and from this moment is maintained between 82 and 85 Pa. To explain this

behaviour is important to emphasize the different silica source and silicon environment used for this solution respect of commercial waterglass solution. In previous studies Torres-Carrasco et al. [15,24] determined by  $^{29}\text{Si}$  NMR that the spectrum for the post treatment liquid, exhibited a single signal at around -71 ppm, associated with the presence of  $\text{Q}^0$  units, i.e., dissolved Si monomers. This is important because according to the literature [43], the effectiveness of Si in waterglass systems rises with declining condensation and polymerization of molecule in the medium. Also the original waste glass have a certain content of impurities that they can react with the basic solution resulting reaction products which can produce changes before reaching a determined value of stress. The initial mechanism of reaction is the same that waterglass solution, producing in this case also the formation of a thin layer of C-S-H gel by the interaction of the silicate ions from solution with  $\text{Ca}^{2+}$  ions form blast furnace slag. However, in this case to 30 minutes of test is not observed significant changes in shear stress.

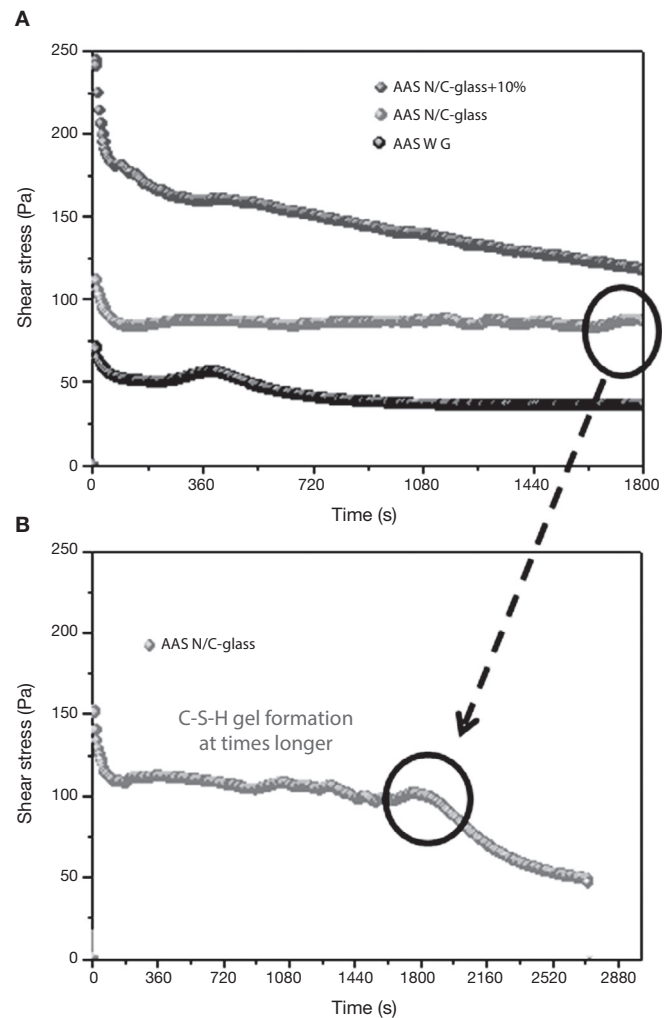


**Fig. 8 – Shear stress in alkali activated slag with different activators: A) AAS WG, AAS N/C-glass and AAS N/C-glass+10%; B) AAS N/C-glass+10% at times longer.**



The main reason of this behaviour is the different source of silicon, due to in this case, the silicon is from waste glass [44].

In order to check if the primary C-S-H gel is formed in this paste at longer times (Fig. 8B), the test was prolonged for 40 minutes at the same rotational speed of  $100 \text{ s}^{-1}$ . As occurred in the slag paste activated with waterglass solution, in this case a signal is also observed around 1800-2000 seconds, after which the stirring conditions of the test break the structure of flocs and descending the values of shear stress to these remain constant. It is confirmed that the activating solution from the waste glass generates primary C-S-H gels longer than commercial waterglass activators.

Finally, when the activating solution was  $\text{NaOH}/\text{Na}_2\text{CO}_3$  after solubility process of waste glass and with 10% substitution of slag by the residual glass waste (solid residue) from solution process (AAS N/C-glass+10%), the rheological performance of this paste is quite different than all other, with a constant decreasing in shear stress values constant during the test. In this case a constant value of the shear stress is not

reached. In these trials, although the test was repeated four times, was not achieved in either case homogeneous value, observing heterogeneous stress values between 250-100 Pa. This behaviour is probably due to the replacement of blast furnace slag by residual glass waste (solid residue). This partial replacement appears to inhibit or delay the reaction between the slag and the activator without the apparent formation of primary mentioned C-S-H gel in testing time. In any case, this inhomogeneity shows that these pastes are not viable from a rheological standpoint for their use, at least in pastes.

#### Determination of rheological parameters: yield stress

In the hysteresis cycles of standard cements (Fig. 9A) follow a straight line with a rise in the early parts of the cycles and a decrease in the final stages of the same after reaching the maximum speed of  $100 \text{ s}^{-1}$ . It is demonstrated the linear relationship between the rotational speed and the shear stress

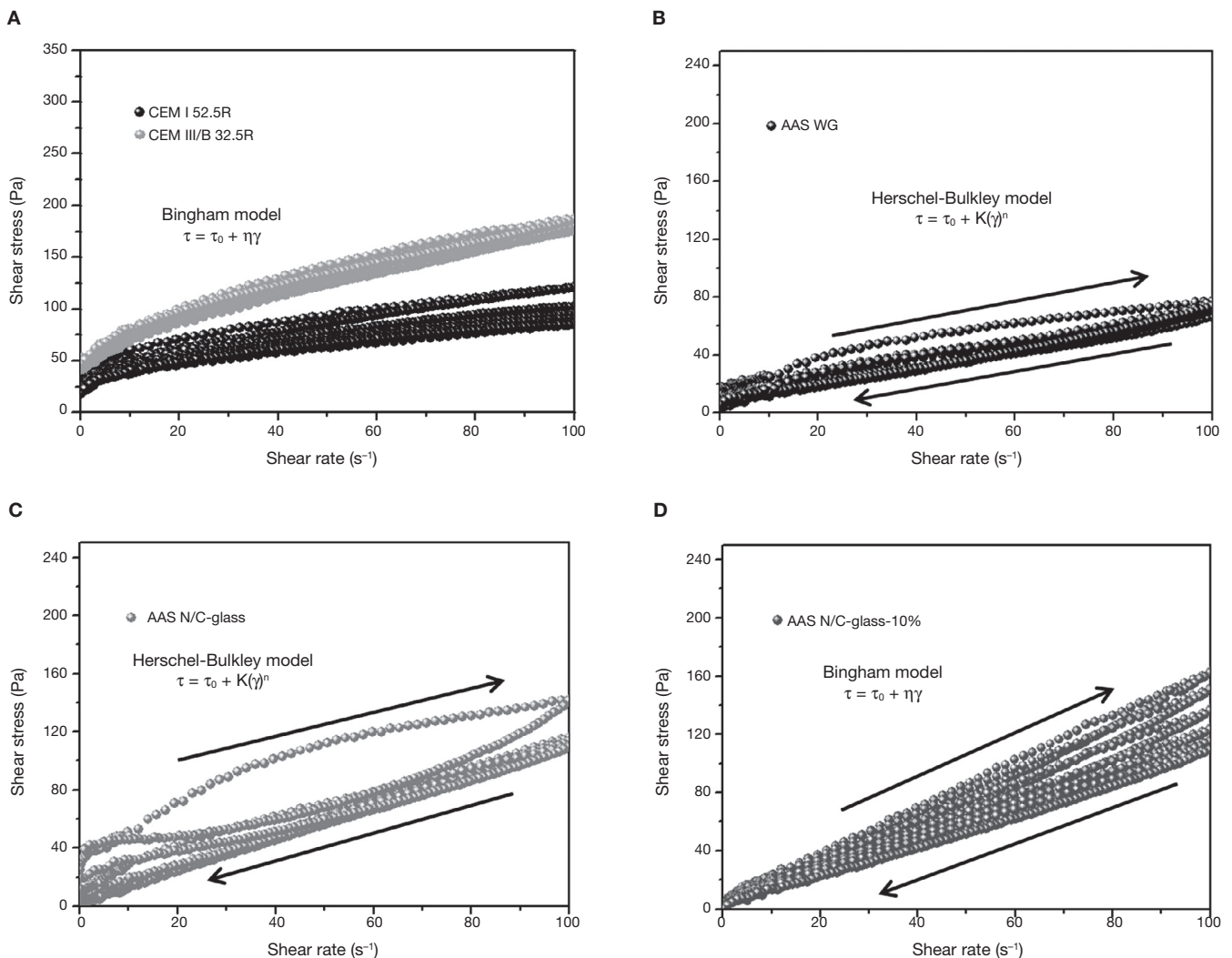


Fig. 9 – Pastes hysteresis cycles: A) CEM I 52.5R and CEM III/B 32.5R; B) AAS WG; C) AAS N/C-glass; D) AAS N/C-glass+10%.

and thus, the possibility of using the Bingham model (Eq. 1) to characterize these materials.

On the other hand, emphasizes the great similarity between the hysteresis cycles of the alkali activated slag with waterglass (Fig. 9B) and the alkali activated slag with NaOH/Na<sub>2</sub>CO<sub>3</sub> and with the waste glass (Fig. 9C). In previous studies [28,39,41,42] have been shown that the rheological behaviour of alkali activated pastes with waterglass is adjusted to Herschel-Bulkley model (Eq. 2). In this study it was found that when the activator comes from the solubility process of waste glass, the model that explains the rheology of their pastes is also Herschel-Bulkley.

$$\text{Bingham model: } \tau = \tau_0 + \eta\dot{\gamma} \quad (1)$$

$$\text{Herschel-Bulkley model: } \tau = \tau_0 + K(\dot{\gamma})^n \quad (2)$$

As to the mixture with partial substitution of slag by attack waste glass (AAS N/C-glass+10%), the hysteresis cycles show a behaviour comparable to standardized cements (Fig. 9D). The most likely cause of this behaviour is the absence of reaction during the process. When the slag is replaced by waste residue, the latter have prevented the activation of the slag was developed, thereby obtaining results similar to those of standard cements hysteresis cycles. Again the results denote heterogeneity. The rheological behaviour of these pastes fits better to Bingham model.

In Figure 10 the results of the shear stress values of standardized pastes and alkaline pastes are shown. In the case of CEM I 52.5R the values of shear stress registered remain constant around 50-55 Pa. The defloculation during the test explains that the effort remains constant. These results are consistent with results obtained by other authors [29,30] and with the results of constant shear rate. However, CEM III/B 32.5R pastes present higher values of shear stress due to the morphology of the slag. In this case, the shear stress values

are around 75-80 Pa, and again, the defloculation test explains this behaviour constant of stress values.

Figure 10B shows the behaviour of the shear stress for alkali activated slag pastes with different activator solutions. When slag is activated with commercial waterglass solution (AAS WG) an increase in the value of stress is produced in the second cycle (25 Pa) and later decrease the values in the third cycle (15 Pa), representing a decrease of 40% and kept constant the rest of the trial. These changes in the values of shear stress are consistent with the behaviour of this paste to constant speed (see Figure 8). In both studies is observed an increase of stress between 5-10 minutes due to hardening of the paste suffered associated with the formation of a primary C-S-H gel.

The behaviour that the slag paste describes when the activator was NaOH/Na<sub>2</sub>CO<sub>3</sub> with the waste glass (AAS N/C-glass) is different when the activator was a commercial waterglass solution being the changes in the stress shear values more prominent. Importantly, the results obtained in these pastes a clear increase in stress values from the fourth cycle is observed, which suggests that from that moment the paste hardens reaching a value of 52.8 Pa, a very high effort to be an alkali activated slag. It seems clear that the increase in yield stress values in the last cycles correspond to the formation of a primary C-S-H gel, appearing delayed with regard to activated slag paste with waterglass solution and with more intensity, mainly due to the difference source of origin of both activators.

Finally, when the slag is activated with NaOH/Na<sub>2</sub>CO<sub>3</sub> after treatment of waste glass and with 10% of replace of the slag by attack waste glass, again the variability is very high in all tests performed in these pastes. We can say like in the previous case that no reaction between the slag and the alkaline solution due to the partial substitution of the slag by attack waste glass. The lack of reaction of the slag causes a constant decrease in the shear stress without changes observed like in the other two alkaline pastes by the formation of primary C-S-H gel.

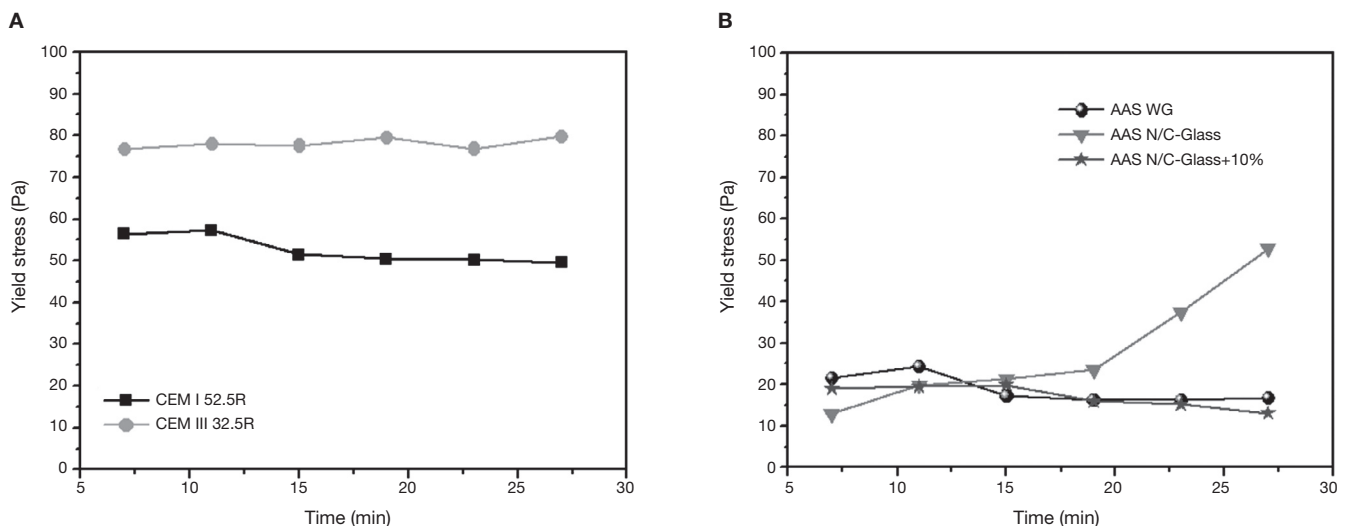


Fig. 10 – Yield stress in A) CEM I 52.5R and CEM III/B 32.5R; B) AAS WG, AAS N/C-Glass and AAS N/C-Glass+10%.

### Paste fluidity (minislump test)

Figure 11 reflects the behaviour of all cement pastes analyzed, taking four measurements at each measurements times in order to highlight the differences in the behaviour of the same pastes, especially between standard cement pastes (CEM I 52.5R and CEM III/B 32.5R) and blast furnace slag pastes activated with different activators.

Regarding the results for CEM I 52.5R pastes, it appears that the fluidity of the cement paste is constant over time since the diameter of the mix remains constant throughout the test. This is also consistent with the shear stresses values analyzed. The presence of a high percentage of addition of slag in the CEM III/B 32.5R not supposed a excessive change in the fluidity respect to CEM I 52.5R pastes, although this is slightly larger at all times. As in the case of CEM I 52.5R pastes, the fluidity of CEM III/B 32.5R remains constant during the test period.

The behaviour after mixing of the slag with any alkaline activator is very different from the standard cements, especially in the early stages of testing cements. For the testing of 5 to 7 minutes there is an average size difference of mix between the standard pastes and the alkaline systems around 28%.

With the commercial waterglass solution the slag pastes show a complex and changing behaviour in the first moment after mixing. In the early stages of testing, we found a very fluid paste with high values of diameter, reaching 126 cm and 129 cm after the first 5 to 7 minutes of the test. After this first trial, the change in the fluidity of the paste is huge (there is a decrease of 21% of the diameter of the mix), reaching values close to those obtained in standard cement pastes at 15 minutes. Subsequently, the mix diameter continues to decrease but in a way much less significantly. We can say that the behaviour of the paste after 15 minutes remains constant from a viewpoint of fluidity. As in previous trials the formation of primary C-S-H gel produced a change, in this case the change more important occurred between 7 and 15 minutes. In this static test the formation and subsequent break in the primary C-S-H gel is later than in the rheological test at share rate (constant speed). The reason of this delay is the simple fact that in this trial did not submit to the paste to any effort after mixing, do not break the primary gel and therefore the gel causes a hardening of the paste and thus a decrease values in the fluidity.

When the solution was used NaOH/Na<sub>2</sub>CO<sub>3</sub> with the waste glass, the initial behaviour of the activated slag paste was very similar to the activated slag paste with commercial waterglass solution. The main difference observe is that the change in the fluidity of the pastes is in this case later and steeper than in slag activated with waterglass solution (in this case the reduction in the diameter values of the mix was 25% between 7 and 30 minutes). As in the previous case, the behavior remains constant after this change in the fluidity, although in this case the stability is not reached until mix measurement at 30 minutes. This late behaviour respect to the alkali activated slag paste with waterglass solution was reflected in the constant share rate, being the most likely cause the diferente nature of the silica may have a less reactive behaviour at early times [15,24].

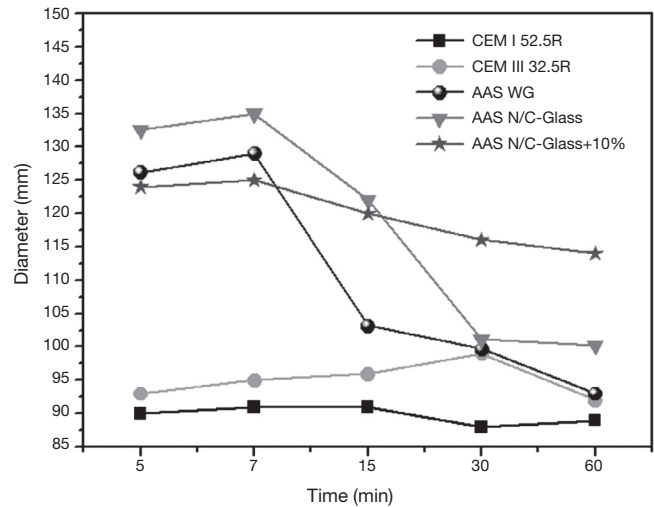


**Fig. 11 – Minislump values for standard cements and AAS pastes with different activators.**

Finally, the behaviour of slag activated with the solution from the waste glass and 10% replacement the blast furnace slag by residual glass waste changed respect to the previous two, where here the fluidity low gradually causing that if the test will lengthen, testing diameters of the mix be achieved close to those of standard cements. As discussed in the previous sections the main problem of this paste is the lack of homogeneity in the mixture of the blast furnace slag with the attack waste glass from the reaction between the waste glass and NaOH/Na<sub>2</sub>CO<sub>3</sub> solution. This inhomogeneity does not allow that the activation of the slag takes place as in the other two alkaline pastes.

## Conclusions

The key conclusions to be drawn from the present study are listed below:

- The data presented here will be valuable in the design and development of high-performance, durable pastes based on alkali-activated slag materials with waste glass as activator, and in the selection and application of appropriate testing methodologies for these materials so the use of waste glass is a good alternative to traditional or conventional activators.
- The rheological differences observed in the different tests between the standard cements and the alkaline cements are due to the formation of the primary C-S-H gel in the latter. It is found that this gel formation is a change in the properties of pastes during the times of measured tests, however, standardized cements show a strong stability in all trials.
- It is demonstrated the feasibility of the standard cements due to the degree of stability shown by both, essentially through the Minislump test. For alkali activated slag pastes with waterglass solution (AAS WG), it is evident that the fluidity change, with a hardening at 15 minutes which can be a problem for its using in the construction. One solution

- to this might be to provide a longer mix to break the gel or introduce some substance to delay the formation of primary C-S-H gel. In any case, the values of fluidity are similar to Portland cements, so workability would be acceptable.
- d) To analyze the feasibility of pastes which incorporating waste glass to its possible use and application in construction, we must differentiate between the solution from waste glass after the solubility process (AAS N/C-glass) and the system which replaced the slag by residual glass waste (AAS N/C-glass+10%), using the same activating solution (NaOH/Na<sub>2</sub>CO<sub>3</sub>). As to the first, the variation in shear stress at a constant shear rate and with the determination of rheological parameters (yield stress and plastic viscosity) show stability for at least the first 20 minutes of the test. However, when not subjected to this paste to a continued effort (Minislump test) occurs a major change in their fluency in just 7 minutes test. Despite showing a significant change in the values of fluidity, the final values provide sufficient fluidity for good workability (very similar values to those of standard cements values). Furthermore yield stress obtained and the shear stress at constant speed ensures that the reaction between the blast furnace slag and the alkaline solution have been well developed. As a result of all this, we can conclude that this use of the waste glass may be feasible from a rheological point of view in pastes can be used, therefore, this type of solutions for activation of blast furnace slags are a good alternative to traditional solutions.
- e) For the replacement of the slag by attack waste glass (AAS N/C-glass+10%), all tests show a clear inhomogeneity, possibly driven by the difficult mixing between the attack waste glass and the slag. As a result, the slag is not properly activated resulting a paste shows no stability. We can conclude that due to heterogeneity and lack of alkali activation shown in these pastes, this way to use the waste glass is not suitable from a rheological point of view to obtain viable pastes.

## Acknowledgments

The present research was funded by the Ministry of Economy and Competitiveness under projects BIA2010-15516 and BIA2013-47876-C2-1-P and under the CSIC project 200460E065. The authors wish to thank P. Rivilla for her assistance with the rheological analyses and A. Gil for his aid with the laboratory trials.

## REFERENCES

1. A. Hasanbeigi, C. Menke, L. Price, The CO<sub>2</sub> Abatement cost curve for the Thailand Cement industry, *J. Clean. Prod.* 18 (2010) 1509.
2. K.H. Yang, Y.B. Jung, M.S. Cho, S.H. Tae, Effect of supplementary cementitious materials on reduction of CO<sub>2</sub>: Emissions from concrete. *J. Clean. Prod.* (in press) 2015.
3. C. Chen, G. Habert, Y. Bouzidi, A. Jullien, A., Environmental impact of cement production: Detail of the different processes and cement plant variability evaluation, *J. Clean. Prod.* 18 (2010) 478.
4. S. Anand, P. Vrat, R.P. Dahiya, Application of a system dynamics approach for assessment and mitigation of CO<sub>2</sub>: Emissions from the Cement industry, *J. Environ. Manage.* 79 (2006) 383.
5. M.B. Ali, R. Saidur, M.S.A. Hossain, Review on emission analysis in Cement industries, *Renew. Sustain. Energy Rev.* 15 (2011) 2252.
6. C.T. Roadmap, Carbon emissions reductions up to 2050. World business council for sustainable development (WBCSD) and International energy agency (IEA), 2010.
7. T. Boden, G. Marland, B. Andres, Global CO<sub>2</sub> emissions from fossil-fuel burning, cement manufacture and gas flaring: carbon dioxide information analysis center, Oak Ridge National Laboratory, Oak Ridge, Tennessee, U.S.A., 2011.
8. X.F. Zhang, S.Y. Zhang, Z.Y. Hu, G. Yu, C.H. Pei, R.N. Sa, Identification of connection units with high GHG emissions for low-carbon product structure design. *J. Clean. Prod.* 27 (2012) 118.
9. V. Glukhovskiy, Y. Zaitsev, V. Pakhomov, V., Slag-Alkaline cements and concretes structures, properties, technological and economic aspects of the use, *Silic. Ind.* 48 (1983) 197.
10. V. Glukhovskiy, G. Rostovskaja, G. Rumyna, High strength slag-alkaline cements, in 7th International Congress Chem. Cem, Paris, 1980, p. 164.
11. A. Fernández-Jiménez, J.G. Palomo, F. Puertas, Alkali-activated slag mortars. Mechanical strength behaviour. *Cem. Concr. Compos.* 29 (1999) 1313.
12. F. Puertas, Cementos de escorias activadas alcalinamente : situación actual y perspectivas de futuro, *Mater. Construcc.* 45 (239) (1995) 53.
13. M. Palacios, F. Puertas, Effect of shrinkage-reducing admixtures on the properties of alkali-activated slag mortars and pastes. *Cem. Concr. Res.* 37 (2007) 691.
14. F. Puertas, M. Torres-Carrasco, Use of glass waste as an activator in the preparation of alkali-activated slag. Mechanical strength and paste characterisation. *Cem. Concr. Res.* 57 (2014) 95.
15. M. Torres-Carrasco, J.G. Palomo, F. Puertas, Sodium Silicate solutions from dissolution of glass wastes: statistical analysis, *Mater. Construcc.* 64 (314) (2014) e014.
16. A. Palomo, P. Krivenko, E. Kavalerova, O. Maltseva, A review on alkaline activation : new analytical perspectives, *Mater. Construcc.* 64 (315) (2014) e022.
17. A. Fernández-Jiménez, A. Palomo, Composition and microstructure of alkali activated fly ash binder: effect of the activator, *Cem. Concr. Res.* 35 (2005) 1984.
18. A.S. Brykov, V.I. Korneev, Production and usage of powdered alkali metal silicate hydrates, *Metallurgist.* 52 (2009) 648.
19. J. Larosa-Thomson, P. Gill, B.E. Scheetz, M.R. Silsbee, Sodium silicate applications for cement and concrete, in: 10th International Congress on the Chemistry of Cement, Gotheburg, 1997.
20. L.K. Turner, F.G. Collins, Carbon dioxide equivalent (CO<sub>2</sub>) emissions: A comparison between geopolymer and OPC cement concrete, *Constr. Build. Mater.* 43 (2013) 125.
21. F. Puertas, M. Torres-Carrasco, C. Varga, J. Torres, E. Moreno, J.G. Palomo, Re-use of urban and industrial glass waste to prepare alkaline cements, in: 4th International Conference on Engineering for waste and biomass valorization, Oporto (Portugal, Vol. 52), 2012.
22. M. Torres-Carrasco, F. Puertas, M. Blanco-Varela, Preparación de cementos alcalinos a partir de residuos vítreos. Solubilidad de residuos vítreos en medios fuertemente básicos, in: XII Congreso Nacional de Materiales (Alicante), Vol. 35, 2012.
23. F. Puertas, J.J. Torres, M. Torres-Carrasco, C. Varga, Procedimiento para la fabricación de cementos alcalinos a partir de residuos vítreos urbanos e industriales. PCT/ES2012/0704408, 2012.
24. F. Puertas, M. Torres-Carrasco, M.M. Alonso, Reuse of urban and industrial waste glass as novel activator for alkali-activated slag cement pastes: a case study, in: Handbook of alkali-



- activated cements, mortars and concretes, Ed. Woodhead Publishing, United Kingdom, 2014, p. 75.
25. M. Jiang, X. Chen, F. Rajabipour, A.M. Asce, C.T. Hendrickson, D.M. Asce, Comparative life cycle assessment of conventional, glass powder and alkali-activated slag concrete and mortar, *J. Infrastruct. Syst.* 20 (4) (2014), 04014020.
  26. S. Stryczek, A. Gonet, Predicting rheological parameters of slag-alkaline slurries, *Arch. Min. Sci.* 43 (1998) 97.
  27. M. Palacios, F. Puertas, P. Bowen, Y.F. Houst, Effect of PCs superplasticizers on the rheological properties and hydration process of slag-blended cement pastes, *J. Mater. Sci.* 44 (2009) 2714.
  28. F. Puertas, C. Varga, M.M. Alonso, Rheology of alkali-activated slag pastes. Effect of the nature and concentration of the activating solution, *Cem. Concr. Compos.* 53 (2014) 279.
  29. M.M. Alonso, M. Palacios, F. Puertas, A.G. de Torre, M.A.G. Aranda, Effect of polycarboxylate admixture structure on cement paste rheology, *Mater. Construcc.* 57 (286) (2007) 65-81.
  30. T. Vázquez, Estudio de algunos componentes del cemento por Espectroscopía Infrarroja. Monografía del Instituto de Ciencias de la Construcción Eduardo Torroja, Ed. CSIC, Madrid, 1971, p. 297.
  31. H.W. Van der Marel, H. Beutelspachcer, Atlas of infrared spectroscopy of clay minerals and their admixtures, Elsevier Scientific Pub, University of California, 1976, p. 396.
  32. A.G. de la Torres, S. Bruque, M.A.G. Aranda, Rietveld quantitative amorphous content analysis, *J. Appl. Crystallogr.* 34 (2001) 196.
  33. S. Diamond, On the glass present in low-calcium and high-calcium fly ashes. *Cem. Concr. Res.* 13 (1983) 459.
  34. G.J. McCarthy, K.D. Swanson, S.J. Steinw, X-Ray diffraction analysis of fly ash. *Adv X-Ray Anal.* 31 (1988) 331.
  35. M. Van Roode, E. Douglas, R.T. Hemmings, X-Ray diffraction measurement of glass content in fly ashes and slags, *Cem. Concr. Res.* 17 (1987) 183.
  36. C. Shi, K. Zheng, A review on the use of waste glasses in the production of cement and concrete. *Resour. Conserv. Recycl.* 52 (2007) 234.
  37. M. Palacios, Y.F. Houst, P. Bowen, F. Puertas, Adsorption of superplasticizer admixtures on alkali-activated slag pastes, *Cem. Concr. Res.* 39 (2009) 670.
  38. D.L. Kantro, Influence of water reducing admixture on properties of cement paste a miniature slump test, *Cem. Concr. Res.* 23 (1980) 1253.
  39. M. Palacios, P. Banfill, F. Puertas, Rheology and setting of alkali-activated slag pastes and mortars: effect of organic admixture, *ACI Mater. J.* 105 (2008) 140.
  40. Z. Huanhai, W. Xuecuan, X. Zhongzi, T. Minshu, Kinetic study of hydration of alkali-activated slag, *Cem. Concr. Res.* 23 (1993), 1253.
  41. C. Rodríguez-Puertas, Comportamiento reológico y mecánico de pastas y morteros de cementos eco-eficientes. Reutilización de residuos vítreos. Proyecto Fin de Carrera-UPM-CSIC, 2014.
  42. M. Palacios, P. Banfill, F. Puertas, Rheological behavior of alkali-activated cement pastes and mortars. effect of admixtures, *ACI Mater. J.* 105 (2008) 140.
  43. M. Criado, A. Fernández-Jiménez, A. Palomo, I. Sobrados, J. Sanz, Effect of the  $\text{SiO}_2/\text{Na}_2\text{O}$  ratio on the alkali activation of fly ash. Part II:  $^{29}\text{Si}$  MAS-NMR Survey, Microporous Mesoporous Mater. 109 (2008) 525.
  44. S. Wang, K.L. Scrivener, P.L. Pratt, Factors affecting the strength of alkali-activated slag, *Cem. Concr. Res.* 24 (1994) 1033.